

A Thermoreflectance Thermography System for Measuring the Transient Surface Temperature of Active Microelectronic Devices

Pavel L. Komarov, Mihai G. Burzo, and Peter E. Raad

Nanoscale Electro-Thermal Sciences Laboratory, Mechanical Engineering Dept.

Southern Methodist University, Dallas, TX 75275-0337, USA

Phone: (214) 768-3043; Fax: (214) 768-4998; Email: praad@smu.edu

Abstract

This work presents a thermoreflectance thermography system capable of measuring the surface temperature field of an activated complex microelectronic device. The article describes the features of the system, the calibration process, and the data acquisition procedure. The measurement methodology consists of first measuring the coefficient of thermal reflectance for each of the surface materials present and then measuring changes in the surface reflectivity at each point of interest with submicron spatial resolution and better than microsecond temporal resolution. The resulting reflectivity waveforms are combined to obtain a transient temperature field over the scanned area. To demonstrate the method's efficacy, it is applied to quantify the thermal behavior of actual MOSFET devices. In particular, the method is used to differentiate between the transient thermal behaviors of identically activated devices that have been made on two different epitaxial layers, one with natural and the other with isotopically-pure silicon. The results show that the isotopically-pure silicon device runs cooler than the corresponding device made with natural silicon. Having this ability to directly measure the thermal behavior of actual devices made it possible to confirm the authors' previous investigation in which they measured higher thermal conductivity for isotopically-pure silicon by the use of a transient thermo-reflectance method.

Key words: Transient temperature scanning, non-invasive, non-contact, submicron thermography, thermo-reflectance coefficient.

Introduction

Significant advancements in microelectronics have been achieved through increases in the density of elementary transistors coupled with decreases in their physical size. The result has been a dramatic increase in heat densities, making the need for removal of heat generated by various internal system components a major design challenge, particularly since overheating can lead to malfunction, degradation in performance, and loss of reliability. Consequently, the ability to predict thermal behavior in the design phase and to measure transient temperatures of existing devices become essential to smart design and continued advancement in microelectronics. As a result, there is an increased demand for methods to determine the temperature of submicron level features. In order to measure the active junctions of modern devices, a method needs to have superior spatial and temporal resolutions. While contact methods have been and continue to be used, they present the added difficulties of having to access features of a submicron device with an external probe, or in the case of embedded features, fabricate a measuring probe into the device, and then having to isolate and exclude the influence of the measuring probe itself. Even then, since in the case of submicron devices the thermal capacitance of the junction

is extremely small, contact methods cannot be used if accurate measurements are desired. Consequently, non-contact, optical methods are usually preferred.

Among the various optical methods, the thermoreflectance method possesses important advantages and is so far one of the methods that has been employed to make submicron temperature mappings [1-6]. The thermo-reflectance thermography (TRTG) is a cost-effective, non-contact and non-destructive optical approach for probing steady-state and transient surface temperature, providing accurate results for submicron features of microelectronic devices with excellent spatial and thermal resolution (better than infrared systems). Also, thermoreflectance-based systems does not suffer many drawback inherent to infrared systems (since is based on the black body radiation emission of the sample). This above drawback makes the infrared measurement systems impossible to use at low temperatures while the thermoreflectance technique will provide excellent results.

Thermoreflectance microscopy is based on the fact that a change in the temperature of a given material produces a small change in the reflectivity of that material's surface. Based on experimental data, the relationship proved to be linear (expanding $\Delta R/R$ as a function of temperature in a Taylor series

expansion and using the experimental results, one can prove that the higher order terms of the expansion are negligible for finite small temperature intervals close to room temperature). Thus, to measure the increase (or decrease) in the temperature of a sample, $\Delta T = C_{TR}^{-1} \Delta R/R$, one needs to measure the change in the reflectivity of the sample $\Delta R/R$ and the thermorelectance calibration coefficient C_{TR} . As one might imagine the most challenging aspect for thermorelectance measurements is the small value of the thermorelectance coefficient of the top layer material, C_{TR} , which defines the rate of change in the surface reflectivity as a function of the change in surface temperature, i.e., $C_{TR} = R^{-1} dR/dT$. The C_{TR} coefficient needs to be sufficiently high in order to obtain an appropriate signal-to-noise ratio in the measurements. Usually, it must be higher than 10^{-5} per Kelvin for thermorelectance temperature measurements to be obtainable with good accuracy. The most important factors that influence C_{TR} are the material under test, the wavelength of the probing laser [7-10], and the composition of the sample (if multi-layered) [7, 11, 12].

The main purpose of this article is to introduce the features of the authors' TRTG system and to demonstrate its capabilities by scanning the active area of typical MOSFET devices. The authors had previously measured [13, 14] the thermal conductivity of isotopically-pure and natural silicon using the transient thermorelectance method. Their results indicated a gain of approximately 55% in the thermal conductivity of Si^{28} as compared to that of natural Si. Therefore, it was anticipated that a MOSFET device constructed using a Si^{28} substrate will run cooler than one built on natural Si. In this work, the TRTG system is used to validate the observed differences by directly probing the transient thermal behaviors of identically activated devices that have been made on two different epitaxial layers, one with natural and the other with isotopically-pure silicon. The system's efficacy is shown through the fact that it makes it possible to measure the resulting transient thermal behavior and ascertain unequivocally whether the Si^{28} device indeed runs cooler than the Si device as should be expected.

Experimental Methodology

This section describes the features of the experimental setup, provides details of the calibration process used to map the changes in the measured surface reflectivity to absolute temperature values, and explains the data acquisition procedure used to measure the transient temperature over a given active region with minimum random noise.

Experimental Setup

The newly-built TRTG experimental system at the SMU NETS Laboratory is depicted schematically in Fig. 1. The probing light source is an Ar-Ion CW laser with a linearly polarized, single-mode ir-

radiation beam at a wavelength of 488 nm. The beam is delivered to the microscope assembly via a polarization preserving, fiber optic cable with TEM_{00} mode. Delivering the probing laser energy by a fiber makes it possible to easily incorporate lasers of different wavelengths to maximize the C_{TR} . This is an important issue since, as shown by Tessier et al. [7], the C_{TR} of a specific material is extremely sensitive to the wavelength of the laser and varies strongly between materials. The data presented for Al, Au, Cu, and Ni by Rosei and Lynch [8], Hanus et al. [9], and Scouler [10] confirm the fact that the C_{TR} coefficient is wavelength dependent.

The microscope objective lens focuses the laser light perpendicularly to the device under test (DUT). The probing beam reflects from the heated surface back along the optical path to the sensitive area of a photodiode (PD1 in Fig. 1). The intensity of the reflected light depends on the reflectivity (temperature) of the sample's surface. The photodiode signal, containing the change in surface reflectivity caused by the temperature variations of the DUT, is acquired with an 8-bit resolution via a digital oscilloscope at a rate of up to 2 Giga-samples per second. This sampling rate allows the measurement of a transient temperature field of a DUT activated in the pulse mode with frequencies of up to 50 MHz, which provides 40 data points to amply describe a full heating and cooling cycle.

The integrated microscope and CCD camera system is mounted on a Cascade Microtech Alessi precision probing station, making it possible to view the DUT and to position the laser beam on its surface with a submicron resolution. The smallest probing spot that can be achieved with the current system and a 100X objective lens is $0.7 \mu\text{m}$.

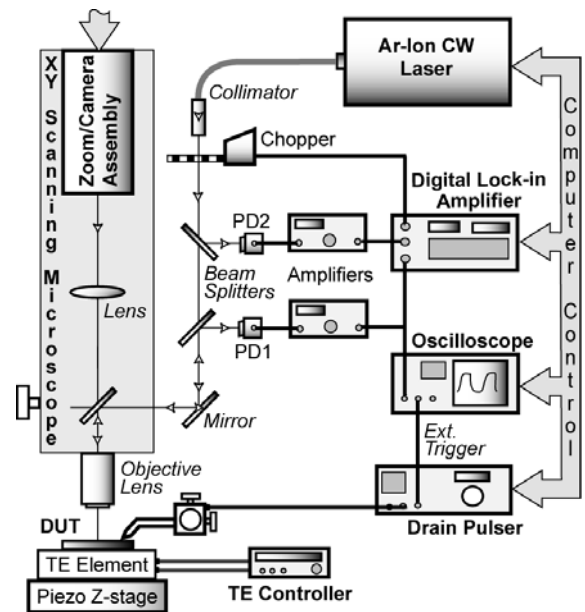


Figure 1: Schematic of the TRTG experimental setup (scanning and C_{TR} calibration)

Calibration procedure

To minimize parasitic effects associated with the thermal expansion of the DUT heater/holder, a small (30×30×5 mm) thermoelectric (TE) device was used to calibrate the measurements. The calibration approach consists of determining the dependence between the change in the reflectance and the change in the surface temperature. The change in reflectance was measured by a differential scheme involving two identical PDs, two pre-amplifiers and a digital lock-in amplifier, in order to increase the signal to noise ratio to be able to measure the small values of the thermoreflectance coefficient. In this approach, the laser light is divided into two beams, one collected on the reference PD2 and the other collected on the photodetector PD1 after being reflected from the sample surface. The signals from the two photodetectors are equalized by controlling the light collection on the reference photodetector through optical attenuation (carried out by precise rotation of a Glan-Taylor polarizer). The sample temperature is measured with a K-type thermocouple positioned on the top surface of the sample. The calibration must be performed for each of the materials on the surface of each device where a mapping of the temperature is carried out.

The reflectance coefficient is normally very small (on the order of 10^{-4} for gold covered with a silicon oxide passivation layer [7, 15]), and therefore parasitic effects must be minimized in its measurements. Dilhaire et al. [15] have pointed out that the thermoreflectance calibration procedure can be hindered by the movement of the device under test as a result of the thermal expansion of the heater. The movement generates both interferometric and out-of-focus parasitic effects in the photodetector signal. Given the potential negative implications of the aforementioned parasitic effects, tests were designed and carried out to help assess the magnitude of these effects in the present system. As expected, our tests showed that measurements with a high numerical aperture (NA) objective are more sensitive to the out-of-focus effect than those with a low NA lens. Thus, we minimized the out-of-focus effect in our system by using only low NA objective lenses. We also investigated the presence of parasitic interferometric effects, and, unlike in the case of the system reported on by Dilhaire et al. [15], did not detect any in the PD signal for the objective lens used.

Temperature Data Acquisition

Extracting the temperature value at a given point on the surface of an active device in the framework of the thermoreflectance method requires the measurement of the surface reflectivity at that point. This can be achieved by capturing on the photodetector the level of laser energy reflected back from the sample and scaling it with the calibration data (C_{TR}). However, given the small value of the coefficient of reflectivity, such an approach would have a very weak signal-to-noise ratio. To overcome

this limitation, the activation voltage of the device is pulsed, resulting in a modulated photodetector signal. This signal is acquired by the oscilloscope, which is triggered at the same phase as the drain pulser activation voltage. The outcome of each data collection after a pulsed activation is a transient waveform, an example of which is drawn with open diamond symbols in Fig. 2, superimposed on the modulated activation voltage (dashed line). After averaging over 256 phase-locked waveforms captured by the oscilloscope, each containing 500 data samples, the transient reflectivity signature at a physical location (as shown in Fig. 2) is obtained with good accuracy (in the range of 1 to 2%). Once the reflectivity is measured, the corresponding absolute temperature value can be calculated by scaling with the thermoreflectance coefficient.

The temperature field over a region of interest can be mapped by repeating the above procedure at multiple physical locations. The SMU thermography scanning system is designed to acquire the temperature at a point, which can be positioned with a resolution of 0.5 μm (in the x and y directions), and then automatically repeat the process over a grid covering the physical region of interest. This scanning process yields a transient temperature field over the desired surface area with a submicron spatial and sub-microsecond temporal resolution.

While the extent of the region of interest and the number of measurement points in it can be specified, acquisition time is a limiting factor. Presently, the system can generate the averaged temperature waveform (shown in Fig. 2) at a physical location in approximately 9 seconds. The use of photodetector arrays and faster multi-channel parallel post-processing can potentially speed up the measurements by at least two orders of magnitude.

Results and Discussion

Two temperature scanning experiments were conducted on typical MOSFET devices which were built on either natural Si or isotopically pure Si epitaxial layers. The devices were geometrically identical and were activated in pulsed mode. A top view of a scanned device is shown on the bottom of Fig 3.

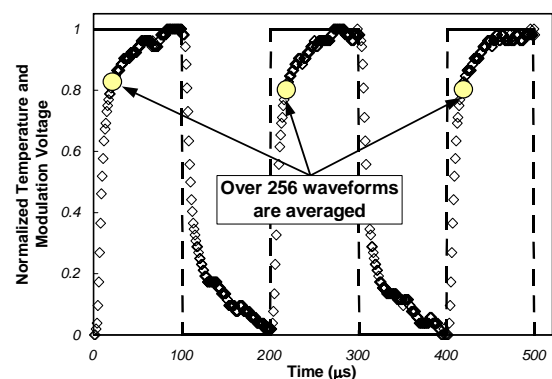


Figure 2: Transient normalized temperature (open squares) and modulation signal (dashed line), shown at hottest point on MOSFET device.

In scanning across the channel from drain to source, for example, the probing laser detects the signal from several different materials including aluminum, silicon, and polysilicon. As previously discussed, the thermorefectance coefficient differs between these materials, leading to different measurement signal levels. With the oscilloscope's 8-bit resolution, the polysilicon covered region yielded data with the requisite level of accuracy. This is consistent with expectations since polysilicon has a superior C_{TR} value (order of 10^{-3}) to even that of silicon (order of 10^{-4}) [5, 6, 12] or contact metal (order of 10^{-5}) [6].

Two identical devices, one built on a natural Si epitaxial layer and the other on isotopically pure Si epitaxial layer were activated and scanned. The scanned area of $23 \times 15 \mu\text{m}$ includes the channel of the MOSFET devices. At each measurement location, 256 waveforms of the photodetector signal were averaged in order to reduce the random noise inherent in the system. Since the overall sampling capability of the system is more than 50 MHz (20 ns) and the timescale of the heat transfer (conduction) in microelectronic devices is usually in the microseconds (and up to milliseconds), the system has sufficient time resolution to capture the fastest possible heating/cooling processes. This fast temporal capability of the thermorefectance temperature scanning system is evident graphically in the temperature waveform shown in Fig. 2. The full heating and cooling cycle in this case takes around 0.2 ms.

The scanned area on the two identical devices is delineated by a black rectangle in Fig. 3. The measured temperature contours are shown at the

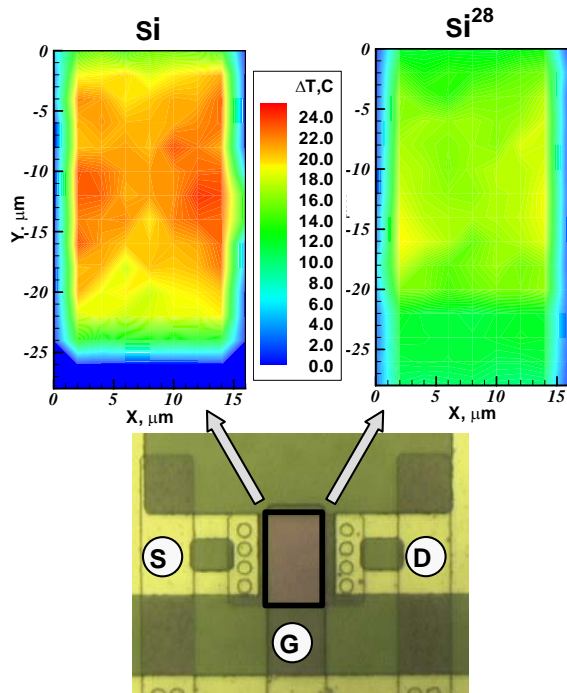


Figure 3: Scan Area and corresponding temperature contours on an activated MOSFET device at the time of peak temperature (channel dimensions are $15 \times 23 \mu\text{m}$)

time when both devices have reached their respective peak temperatures. The electric current used to activate this device was pulse-modulated at 5 KHz and 50% duty cycle. To produce the absolute temperature rise values plotted in Fig. 3, the measured reflectivity field was scaled with the experimentally obtained thermorefectance coefficient. The latter was measured as described in the previous section but with a 10X objective lens in order to eliminate the out-of-focus parasitic effect. As expected, the measurements presented in Fig. 3 show that the device built on Si^{28} runs cooler than the one built on natural Si (by approximately 20%).

The transient surface temperature behaviors of the Si and Si^{28} based MOSFET devices are presented in the upper and lower parts of Fig. 4, respectively, as snapshots of temperature contour animations. The eight snapshots represent the surface temperature field at different instances in the heating and cooling phases of the full pulsed cycle. The times during the cycle are identified as circled numbers both on the contour plots and on the waveform graph shown in the central part of Fig. 4. The snapshot times were chosen to graphically represent the transient thermal behavior of the MOSFET devices. This approach can provide equally rich understanding of the transient thermal behavior of devices that are operated at much higher pulse rates and/or at other duty cycles.

The results obtainable through the use of the thermorefectance temperature scanning system would make it possible for analysts and designers of both existing and next generation devices to make decisions that are based on actual behavior as opposed to approximate simulations or reduced-order models. And, even when the latter simulations and models are available and their use is desirable, direct measurements can be invaluable in validating the results of such computational techniques and substantiating the consistency of such models.

Conclusions

In this article, a new TRTG experimental system has been presented and used to scan the surface temperatures of representative MOSFET devices. The system is ideally suited to non-invasively and non-destructively measure the surface temperature field of devices undergoing the ultrafast transients that are typical of next generation microelectronic devices. Specifically, we have demonstrated that the system is capable of capturing the thermal transients of a device pulsed at speeds of up to 50 MHz, which far exceed the physical scales of temperature response. When using a 488 nm Ar-Ion laser, the system provides a submicron, diffraction-limited, spatial resolution. The system's efficacy was demonstrated by presenting the results of surface temperature scans of pulsed MOSFET devices constructed on two epitaxial layers, one on a natural Si layer and another on the 55% more thermally conductive isotopically pure Si^{28} layer.

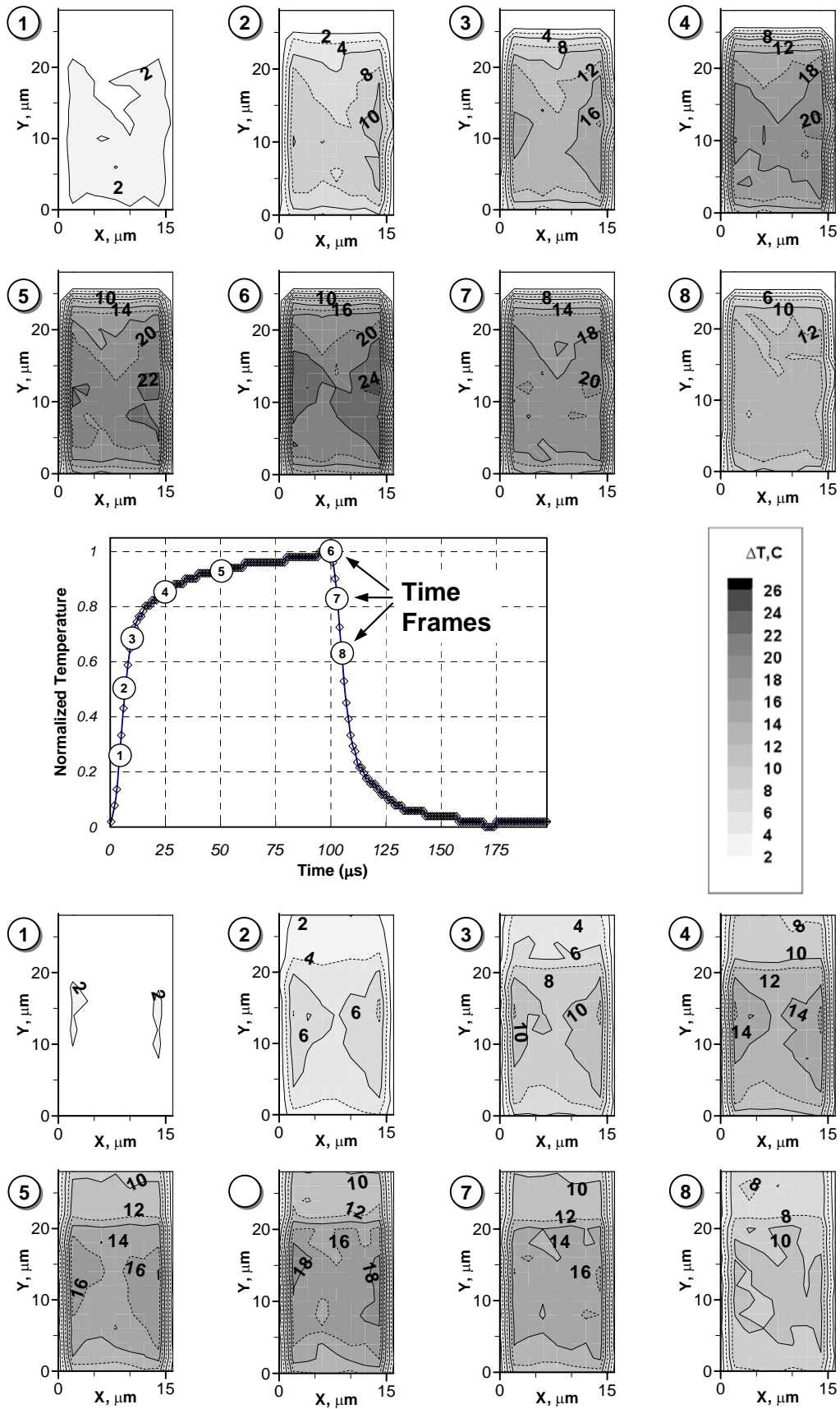


Figure 4: Temperature contours for activated devices (Si on top two rows and Si^{28} on bottom two rows) during a pulse cycle. The time frames are identified in the central plot by circled numbers on the normalized temperature wave form.

The results show non-negligible differences in the resulting transient temperature signatures due to the use of different materials in the construction of the otherwise identical devices, with the isotopically-pure silicon device running approximately 20% cooler than the corresponding device made with natural silicon. This measured behavior provides confirmation of the authors' previous measurement of higher thermal conductivity for isotopically-pure silicon. Accounting for the uncertainties associated with the calibration (i.e., obtaining C_{TR}) and the actual temperature scanning, the overall random uncertainty of the results is estimated to be less than 13%.

The ultimate power of a direct thermography approach is as a part of an integrated approach whose aim is to characterize the transient thermal behavior of fully-featured three-dimensional (3D) structures. The overall approach would use the described experimental technique to non-invasively scan the surface temperature where possible and then would solve an inverse numerical problem with an ultra-fast adaptive technique to determine the temperature distribution over the entire 3D device, including important embedded features whose response is otherwise impossible to measure directly.

Acknowledgments

The authors are grateful to Prof. Sanjay Banerjee and his research assistant Lisa Weltzer of University of Texas at Austin for providing the MOSFET devices.

References

- [1] K.E. Goodson and Y.S. Ju, "Short-time-scale Thermal Mapping of Microdevices using a Scanning Thermoreflectance Technique," *ASME Journal of Heat Transfer*, Vol. 120, pp. 306-313, 1998.
- [2] S. Grauby, S. Hole, and D. Fournier. "High Resolution Photothermal Imaging of High Frequency Using Visible Charge Couple Device Camera Associated with Multichannel Lock-in Scheme," *Review of Scientific Instruments*, Vol. 70, No. 9, pp. 3603-3608, 1999.
- [3] V. Quintard, S. Dilhaire, T. Phan, and W. Claeys, "Temperature Measurement of Metal Lines under Current Stress by High Resolution Laser Probing," *IEEE Transactions on Instrumentation and Measurement*, Vol. 40, pp. 69-74, 1999.
- [4] Z. Bian, J. Christofferson, A. Shakouri, and P. Kozodoy, "High-power operation of electroabsorption modulators," *Applied Physics Letters*, Vol. 83, pp. 3605-3607, 2003.
- [5] S. A. Thorne, S. B. Ippolito, M. S. Ünlü, and B. B. Goldberg, "High-resolution thermoreflectance microscopy," *Materials Research Society Proceedings*, Vol. 738, November 2002.
- [6] J. Christofferson, D. Vashae, A. Shakouri, P. Melese., F. Xiaofeng, Z. Gehong, C. Labounty, J.E. Bowers., E.T. Croke, III. "Thermoreflectance Imaging of Superlattice Micro Refrigerators," *Seventeenth Annual IEEE Semiconductor Thermal Measurement and Management Symposium*, San Jose, CA, pp. 58-62, 2001.
- [7] G. Tessier, S. Hole, and D. Fournier, "Quantitative Thermal Imaging by Synchronous Thermoreflectance with Optimized Illumination Wavelengths," *Applied Physics Letters*, Vol. 78, pp. 2267-2269, 2001.
- [8] R. Rosei, and D.W. Lynch, "Thermomodulation Spectra of Al, Au, and Cu," *Physical Review B*, Vol. 5, pp. 3883-3893, 1972.
- [9] J. Hanus, J. Feinleb, and W.J. Scouler, "Low-energy Interband Transitions and Band Structures in Nickel," *Physical Review Letters*, Vol. 19, pp. 16-20, 1967.
- [10] W.J. Scouler, "Temperature Modulated Reflectance of Gold from 2 to 10 eV," *Physical Review Letters*, Vol. 18, pp. 445-448, 1967.
- [11] V. Quintard, G. Deboy, S. Dilhaire, D. Lewis, T. Phan, W. Claeys, "Laser Beam Thermography of Circuits in the Particular Case of Passivated Semiconductors," *Microelectronic Engineering*, Vol. 31, pp. 291-298, 1996.
- [12] J. Heller, J.W. Bartha, C. C. Poon, and A. C. Tam, "Temperature Dependence of the Reflectivity of Silicon with Surface Oxides at Wavelengths of 633 nm and 1047 nm", *Applied Physics Letters*, Vol. 75, pp. 43-45, 1999.
- [13] P. L. Komarov, M. G. Burzo, G. Kaytaz, and P. E. Raad, "Transient Thermo-Reflectance Measurements of the Thermal Conductivity and Interface Resistance of Metallized Natural and Isotopically-Pure Silicon," *Microelectronics Journal*, Vol. 34, pp. 115-118, 2003.
- [14] M. G. Burzo, P. L. Komarov, and P. E. Raad, "Non-contact Thermal Conductivity Measurements of Gold Covered Natural and Isotopically-Pure Silicon and Their Respective Oxides," 5th Int. Conf. on Thermal, Mechanical and Thermo-mechanical Simulation and Experiments in Micro-electronics and Micro-systems, Brussels, Belgium, May 10-12, 2004.
- [15] S. Dilhaire, S. Grauby, and W. Claeys, "Calibration Procedure for Temperature Measurements by Thermoreflectance Under High Magnification Conditions," *Applied Physics Letters*, Vol. 84, pp. 822-824, 2004.